AIP | Applied Physics Letters

Leakage conduction behavior in electron-beam-cured nanoporous silicate films

Po-Tsun Liu, T. M. Tsai, and T. C. Chang

Citation: Applied Physics Letters **86**, 182903 (2005); doi: 10.1063/1.1921329
View online: http://dx.doi.org/10.1063/1.1921329
View Table of Contents: http://scitation.aip.org/content/aip/journal/apl/86/18?ver=pdfcov
Published by the AIP Publishing

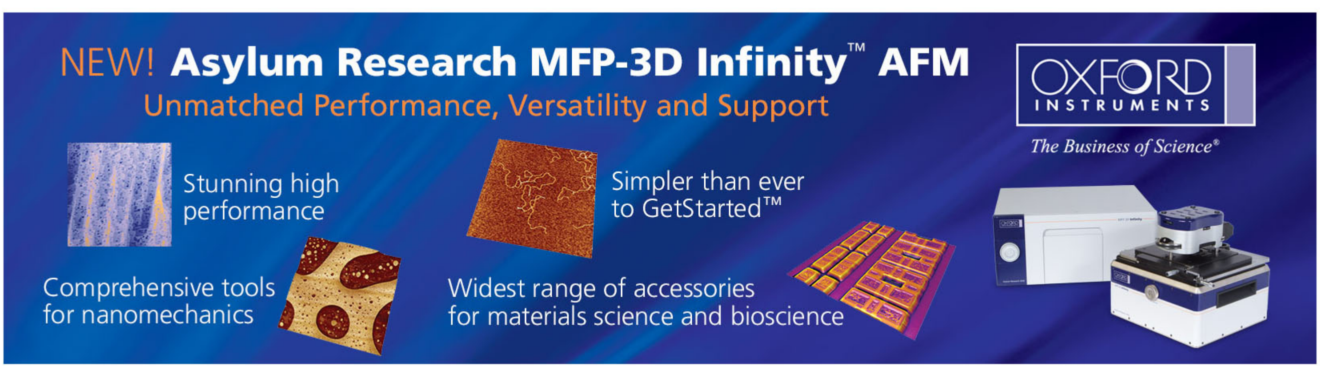

Leakage conduction behavior in electron-beam-cured nanoporous silicate films

Po-Tsun Liu[a)]
Department of Photonics and Display Institute, National Chiao Tung University, 1001 Ta-Hsueh Road, HsinChu 300, Taiwan, R.O.C.

T. M. Tsai
Institute of Electronics, National Chiao Tung University, Taiwan, R.O.C.

T. C. Chang
Department of Physics and Institute of Electro-Optical Engineering, National Sun Yat-Sen University, Taiwan, R.O.C.

(Received 8 November 2004; accepted 15 March 2005; published online 25 April 2005)

This letter explores the application of electron-beam curing on nanoporous silicate films. The electrical conduction mechanism for the nanoporous silicate film cured by electron-beam radiation has been studied with metal-insulator-semiconductor capacitors. Electrical analyses over a varying temperature range from room temperature to 150 °C provide evidence for space-charge-limited conduction in the electron-beam-cured thin film, while Schottky-emission-type leaky behavior is seen in the counterpart typically cured by a thermal furnace. A physical model consistent with electrical analyses is also proposed to deduce the origin of conduction behavior in the nanoporous silicate thin film. © *2005 American Institute of Physics*. [DOI: 10.1063/1.1921329]

During past decades, there has been a great deal of interest in electron-beam (EB) technology applications,[1–4] such as film deposition, material inspection, polymer modification, degradation of pollutants, and especially the field of nanometer scale pattern generation driven by semiconductor technology. Electron-beam lithography is currently one of promising approaches to achieve high-resolution patterning with nanometer scale.[5,6] Additionally, in recent years a lot of research and development activity has been expanded on the use of EB technology for the curing of advanced composites and polymers for the aerospace and electric industries.[6,7] Curing includes the polymerization of monomers or oligomers and cross-linking of polymers. The energy coming from EB radiation is delivered directly to the molecules, thus there is no need to heat the material in ovens, furnaces, or other tools, or to allow for osmosis of chemicals in the material being processed. The EB curing thereby offers several benefits, involving easier material handling, ambient temperature curing, less film stress by temperature differences, and cocuring of dissimilar materials. When performing EB curing on dielectrics applied to integrated circuit (IC) industry, electrical properties of processed dielectric materials will be one of critical considerations.[8] However, few documents have focused on electrical conduction mechanisms of EB-processed materials.[9,10] In our previous work,[11] the direct patterning of silicate thin film has been developed by the use of EB microlithography technology; nonetheless, the details of improved electrical characteristics have not been explored explicitly. This work will extend the electrical study on the leakage behavior of EB-cured nanoporous silicate film by the analysis of current-voltage (*I-V*) curves dependent on temperature. In particular, the leakage transport mechanisms will be clarified by extracting the *I-V* information. The adoption of nanoporous silicate with low permittivity for IC technology can effectively reduce signal propagation delay, power consumption, and enhance circuit performance.[8]

A nanoporous silicate, manufactured by Chemat Technology Inc., was used as an electron-sensitive dielectric material through this study. Methyl silsesquioxane (MSSQ) resin as the matrix material, which is low molecular weight with a large number of $Si(OH)_x$ and $Si(OC_2H_5)_x$ ($x=1-4$) groups, was formulated to 30 wt. % solids in a carrier solvent of methylisobutylketone. Poly(methylmethacrylate) polymers (PMMA) with 20 wt. % loading, working as foaming agents, were subsequently added in the MSSQ matrix material to ultimately produce porous silicate. As most PMMA polymers were compatible with MSSQ, a uniform precursor solution of the mixture was obtained immediately. For fabricating nanoporous silicate films, the precursor solution was first spin-coated onto 6-in. *p*-type silicon wafers with (100) orientation, using two coating stages on a spin coater. In the first stage, spin speed was set 500 rpm and the spinning time was 5 s, beneficial for sequent sol spreading. The second stage (3000 rpm/20 s) was a rinsing step designed to get rid of the edge bead of the precursor, which might induce cracks when drying. After spin deposition, as-spun wafers were followed by baking on a hot-plate at 100 °C for 1 min to remove residual organic solvent in the as-spun nanoporous silicate film. EB blanket irradiating was then carried out to cure the postbaked silicate film coated on the 6 in. silicon wafer, by use of a Leica Weprint200 stepper. The area irradiated by the EB was 182 cm^2 and the thickness of the EB-cured nanoporous silicate film was 450 nm. The EB shape current was 4 A/cm^2 with an accelerating energy of 40 keV, allowing a sufficient curing of the nanoporous silicate film from top to bottom. The exposure doses were changed from 100 to 700 $\mu C/cm^2$. In this work the exposure dosage of 250 $\mu C/cm^2$ was the minimum dose required for achieving an efficient curing. The control samples were also manufactured for comparison, according to a typical commercial recipe shown as follows. The as-spun silicate film on wafers were transferred to a quartz furnace and heated up from room temperature (27 °C) to 425 °C at a ramping rate of 20 °C/min. A thermal curing process then proceeded at

[a)]Electronic mail: ptliu@mail.nctu.edu.tw

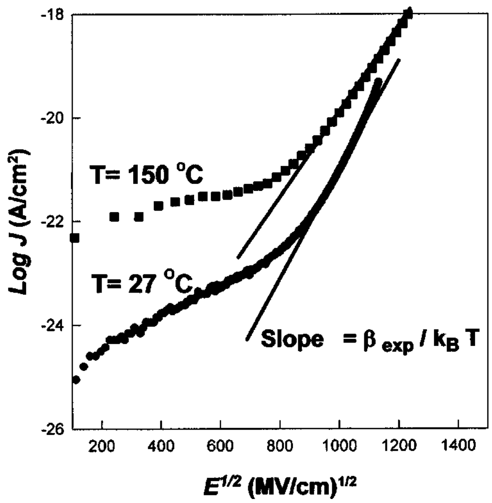

FIG. 1. Log J versus $E^{1/2}$ plot of thermally furnace-cured nanoporous silicate film at the high electric field region, measured at 27 and 150 °C, respectively. The linear relationship of log J-$E^{1/2}$ curves is characterized by Schottky-emission leakage mechanism.

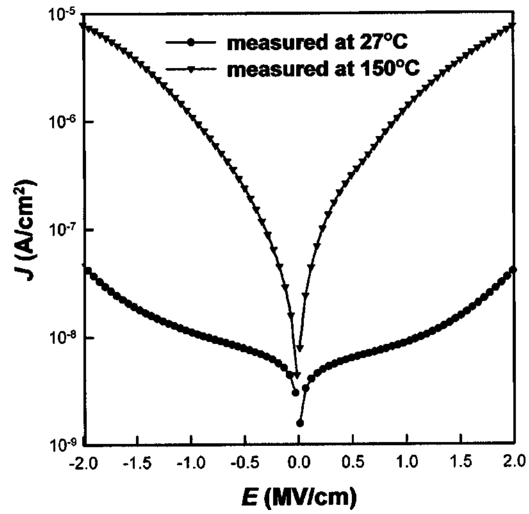

FIG. 2. Leakage current density of electron-beam cured nanoporous silicate film as a function of electric fields, measured at 27 and 150 °C. The symmetry of J-E curves measured from MIS capacitors suggests bulk-dominated conduction behavior.

425 °C for 1 h under nitrogen atmosphere, further forming nanoporous silicate films. Electrical measurements were conducted on metal-insulator-semiconductor (MIS) capacitors by thermally evaporating Al electrodes on the front surface of the nanoporous silicate films and the backside of the silicon wafer. The current-voltage (I-V) characteristics were measured with an HP4156C semiconductor parameter analyzer with the MIS capacitors biased at the accumulation polarity.

In the initial study, the electrical analysis was conducted to characterize the leakage current of nanoporous silicate film typically cured by a thermal furnace. Various conduction mechanisms such as ohmic conduction, Schottky emission, and Poole-Frankel (PF) emission can be demonstrated using MIS capacitors through leakage current density versus electric field (J-E) and log J versus $E^{1/2}$ curve fitting.[12–14] At low electrical fields the leakage current is typical of ohmic conduction, apparently because of thermally generated carriers. This observation has been experimentally confirmed by previous research.[15,16] Moreover, a plot of the leakage current density versus the square root of the applied field gives a good representation of the leakage behavior at high electric fields, as shown in Fig. 1. It is found that leakage current density of the furnace-cured nanoporous silicate film are linearly related to the square root of the applied electric field at 27 and 150 °C, corresponding either to Schottky emission (SE) or to PF mechanism.[12,14] The current density in the SE can be quantified by the following equation:

$$J = A^* T^2 \exp\left(\frac{\beta_{\mathrm{SE}} E^{1/2} - \phi_s}{k_B T}\right) \tag{1}$$

where $\beta_{\mathrm{SE}} = (e^3/4\pi\varepsilon_0\varepsilon)^{1/2}$, e the electronic charge, ε_0 the dielectric constant of free space, ε the high-frequency relative dielectric constant, A^* effective Richardson constant, T absolute temperature, E the applied electric field, ϕ_s the contact potential barrier, and k_{B} the Boltzmann constant. The current density for PF-type conduction is given by

$$J = J_0 \exp\left(\frac{\beta_{\mathrm{PF}} E^{1/2} - \phi_{\mathrm{PF}}}{k_{\mathrm{B}} T}\right), \tag{2}$$

where $J_0 = \sigma_0 E$ is the low-field current density, σ_0 the low-field conductivity, $\beta_{\mathrm{PF}} = (e^3/\pi\varepsilon_0\varepsilon)^{1/2}$, ϕ_{PF} the height of trap potential well.

The two processes can be distinguished by comparing the theoretical values of β_{SE} and β_{PF} with the calculated one obtained from the slope of the experimental curve log J versus $E^{1/2}$.[14] The relative dielectric constant determined from capacitance measurements of samples with the Al-gate electrodes is about 2.2 at 27 °C, and approximately constant at 150 °C. The slope of the straight-line portion of curves in Fig. 1 gives a calculated value of 3.6×10^{-23} J(m/V)$^{1/2}$ at high electric fields for experimental β. The theoretical value of β_{SE} and β_{PF} are 3.7×10^{-23} and 7.4×10^{-23} J(m/V)$^{1/2}$, respectively. From these results, at high electric fields, the leaky transport mechanisms in the furnace-cured nanoporous silicate could be summarized by the Schottky emission. The Schottky emission generated by the thermionic effect is caused by electron transport across the potential energy barrier via field-assisted lowering at a metal-insulator interface.

Measurement of J-E characteristics at varying temperatures is also conducted to clarify the leakage behavior of EB-cured nanoporous silicate film. Figure 2 depicts J-E curves of the EB-cured nanoporous silicate under a voltage sweeping from −50 to 50 V, at different temperatures (27 and 150 °C). It is found the leakage current density is temperature-dependent and increased by nearly two orders of magnitude, when measurement temperatures increase from 27 to 150 °C. In addition, the J-E characteristics exhibit nearly symmetrical and obey a power law relationship over several decades of current, strongly suggestive of space-charge-limited current (SCLC) in the presence of distributed traps.[17,18] This is especially possible for the EB-cured nanoporous film, due to electron-beam irradiation into a relatively loose bonding network of porous silicate. As considering SCLC conduction, the current density can be expressed as the following equation:[19]

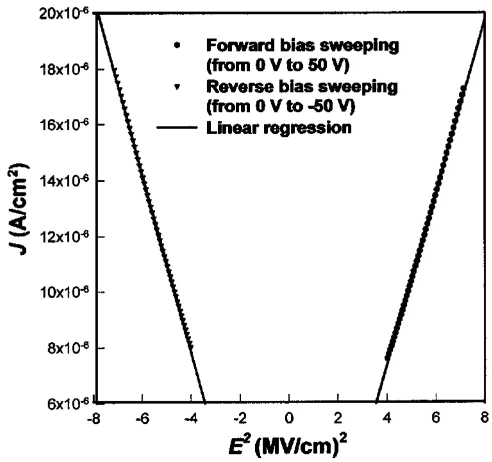

FIG. 3. J versus E^2 plot of electron-beam-cured nanoporous silicate film, measured at 150 °C. The linear relationship of J-E^2 curves indicates the space-charge-limited conduction in EB-cured nanoporous silicate.

$$J = \frac{9\varepsilon_0\varepsilon_r\mu\theta}{8d^3}V^2 \propto E^2,$$

where μ is the free carrier mobility, ε_0 the permittivity of free space, ε_r the relative dielectric constant of the sample material, d the sample thickness, and θ is the ratio of the free charge carriers to trapped ones, which takes into account the trapping center concentration and their distribution. The SCLC conduction are usually interpreted in terms of charge injection and subsequent filling of the trapping centers giving rise to progressively the square-type dependence of the J-E characteristics. To best confirm SCLC conduction, J-E characteristics are transformed into a plot of the leakage current density versus the square of the applied electric field to give a good representation of the leakage conduction behavior, as shown in J-E^2 curves of Fig. 3. It can be observed that the leakage current densities of EB-cured nanoporous silicate film are linearly proportional to the square of the applied electric field, which obeys the SCLC conduction behavior.

We propose the following explanation for the observed leakage behavior of EB-cured nanoporous silicate, and a possible energy band diagram is deduced as displayed in Fig. 4. In this work, the EB curing process can provide a significant amount of energetic electrons injecting into the nanoporous silicate film. A larger fraction of the injection charges are prone to remain in the nanoporous silicate film and form a distribution of space charge layer. The trapping of charges is especially true for the nanoporous silicate film, due to the presence of weak bonds and dangling bonds (or traps) in the loose porous structure. These trapped charges in the nanoporous silicate will induce a field gradient through Poisson's equation, with the result that the electric field is reduced at the cathode (Al electrode) and enhanced in the region between the space charge layer and the anode (Si substrate). This leads the conduction of following charges to obey SCLC behavior. Furthermore, since the occupancy of traps is a function of temperature, the SCLC is temperature dependent.

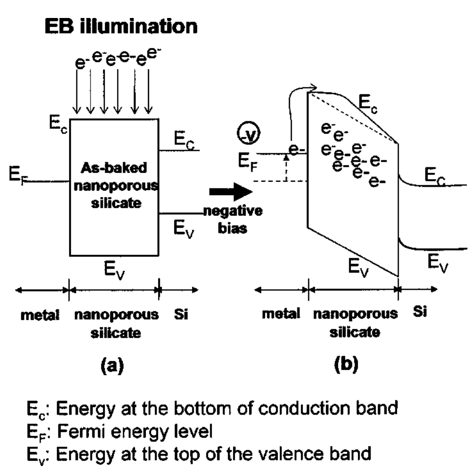

FIG. 4. A proposed energy band diagram of as-baked nanoporous silicate film for SCLC behavior, (a) before and (b) after electron-beam irradiation process.

In conclusion, carrying out electrical analyses at varying temperatures from 27 to 150 °C, we have distinguished the leakage behavior between EB-cured nanoporous silicate film and thermally furnace-cured one. EB-cured nanoporous film exhibits space-charge-controlled conductivity, due to trapped charges in the nanoporous silicate inducing a field gradient during carrier transportation. A proposed energy band diagram is developed to deduce the observed leakage behavior of EB-cured nanoporous silicate. The linear relationship of J versus E^2 curve gives a good confirmation of SCLC behavior. The knowledge of electrical conduction of EB-cured nanoporous silicate can benefit the application of electron-beam technology on the curing of advanced composites and polymers for the aerospace and electric industries.

This work was performed at National Chiao Tung University and National Nano Device Laboratories, Taiwan, R.O.C. The authors would like to acknowledge the financial support of the National Science Council (NSC) under Contract No. NSC 93-2218-E-009-067. In addition, the authors gratefully appreciate the assistance from Dr. C. J. Chu (Nanmat Technology Co. Ltd., Taiwan).

[1] R. Mehnert, Nucl. Instrum. Methods Phys. Res. B **105**, 348 (1995).
[2] T. Djenizian, L. Santinacci, and P. Schmuki, Appl. Phys. Lett. **78**, 2940 (2001).
[3] D. S. Pickard, T. R. Groves, W. D. Meisburger, T. Crane, and R. F. Pease, J. Vac. Sci. Technol. B **21**, 2834 (2003).
[4] P. Visconti, A. Della Torre, G. Maruccio, E. D'Amone, A. Bramanti, R. Cingolani, and R. Rinaldi, Nanotechnology **15**, 807 (2004).
[5] S. D. Berger and J. M. Gibson, Appl. Phys. Lett. **57**, 153 (1990).
[6] A. A. Tseng, K. Chen, C. D. Chen, and K. J. Ma, IEEE Trans. Electron Packag. Manuf. **26**, 141 (2003).
[7] C. Saunders, V. Lopata, J. Barnard, and T. Stepanik, Radiat. Phys. Chem. **57**, 441 (2000).
[8] *International Technology Roadmap for Semiconductors* (Semiconductor Industry Association, Santa Clara, CA, 2001).
[9] R. Manepalli, K. D. Farnsworth, S. A. B. Allen, and Paul A. Kohl, Electrochem. Solid-State Lett. **3**, 228 (2000).
[10] T. Kikkawa, T. Nagahara, and H. Matsuo, Appl. Phys. Lett. **78**, 2557 (2001).
[11] P. T. Liu, T. C. Chang, T. M. Tsai, Z. W. Lin, C. W. Chen, B. C. Chen, and S. M. Sze, Appl. Phys. Lett. **83**, 4226 (2003).
[12] P. T. Liu, T. C. Chang, Y. L. Yang, Y. F. Cheng, S. M. Sze, IEEE Trans. Electron Devices **47**, 1733 (2000).
[13] H. S. Yang, S. Y. Choi, S. H. Hyun, and C. G. Park, Thin Solid Films **348**, 69 (1999).
[14] S. M. Sze, *Physics of Semiconductor Devices* (Wiley, New York, 1981), Chap. 7.
[15] P. T. Liu, T. C. Chang, Y. L. Yang, Y. F. Cheng, J. K. Lee, F. Y. Shih, E. Tsai, G. Chen, and S. M. Sze, J. Electrochem. Soc. **147**, 1186 (2000).
[16] E. R. Neagu and J. N. Marat-Mendes, Appl. Phys. Lett. **82**, 1920 (2003).
[17] M. A. Lampert and P. Mark, *Current Injection in Solids* (Academic, New York, 1970), Chaps. 2, 4, and 5.
[18] S. Ashok, K. Srikanth, A. Badzian, T. Badzian, and R. Messier, Appl. Phys. Lett. **50**, 763 (1987).
[19] T. Iqbal and C. A. Hogarth, Int. J. Electron. **65**, 953 (1988).